ELSEVIER

Journal of Nuclear Materials 240 (1997) 185–195

journal of nuclear materials

The behaviour of single atoms of molybdenum in urania

S. Nicoll [a], Hj. Matzke [a,*], R.W. Grimes [b], C.R.A. Catlow [c]

[a] *European Commission, Joint Research Centre, Institute for Transuranium Elements, P.O. Box 2340, 76125 Karlsruhe, Germany*
[b] *Department of Materials, Imperial College, London SW7 2BP, United Kingdom*
[c] *The Royal Institution of Great Britain, 21 Albemarle Street, London W1X 4BS, United Kingdom*

Received 27 June 1996; accepted 21 October 1996

Abstract

Computer simulation techniques are used to investigate the behaviour of single atoms of Mo in $UO_{2\pm x}$. In UO_{2-x}, Mo is calculated to be present as neutral atoms in bound Schottky trio sites. In UO_{2+x}, most of the Mo is calculated to be in isolated uranium vacancy sites with Mo ionisation increasing with the O/U ratio. The behaviour near stoichiometric composition is more complex and is found to be very sensitive to changes in O/U ratio. An approximation to the free energy change associated with Mo incorporation in urania is plotted as a function of O/U ratio and Mo concentration. Although this plot is found to be in agreement with the observed insoluble character of Mo in urania, at high O/U ratios and very low Mo concentrations, Mo in solution may be preferred over Mo in the gaseous state.

1. Introduction

Of all the fission products Mo occupies a very special place as regards the chemistry of the reactor fuel. Its elemental yield is almost on a par with that of Xe [1] and so its abundance alone would warrant a detailed study of its behaviour. However, unlike the case of Xe, Mo has a major influence on the fuel oxygen potential, $\Delta\overline{G}_{O_2}$, which is of importance for two principal reasons: firstly, it controls the chemical nature of many of the fission products and thereby influences both their physical behaviour and their role in such important factors as fuel swelling and release rates. Secondly, an uncontrolled increase in $\Delta\overline{G}_{O_2}$ may lead to corrosion of the fuel cladding with serious implications for reactor safety and operation. As $\Delta\overline{G}_{O_2}$ is such a major controlling parameter, any factor which modifies it is clearly of great importance.

It is well known (see Section 2) that the oxygen potential of the Mo/MoO_2 couple lies very close to that of stoichiometric UO_2 [1]. The chemical nature of Mo should therefore be a sensitive indicator of fuel stoichiometry and certainly a partitioning of Mo between metallic and oxide phases is observed in reactor fuels [2]. Given its high yield, it is thus clear that Mo may act as a buffer to $\Delta\overline{G}_{O_2}$ and recent measurements in high burn-up fuel suggests this is indeed the case [3].

During the last twenty years, our understanding of the defect properties of UO_2 and of the behaviour of fission products within this material has been greatly illuminated by the application of computer modelling techniques [4–7]. In this paper we give the results of an atomistic computer simulation study into the behaviour of Mo in urania. Our concern is principally with the location and charge state of single Mo atoms in a UO_2 matrix. Possible sites and charge states are investigated through energy minimisation techniques with the effects of Mo concentration and fuel stoichiometry being introduced via a simple mass action type approach. The important question of Mo solubility in urania is also examined using the same methods. Before outlining the computational methods used however, we shall first review what is known experimentally about this important fission product.

* Corresponding author. Tel.: +49-7247 951 273; fax: +49-7247 951 590.

PII S0022-3115(96)00716-7

2. Experimental knowledge

In work reported 30 years ago at Harwell [8] it was recognised that, in irradiated oxide fuels, the noble metals form a separate metallic phase containing the five metals Mo, Tc, Ru, Rh and Pd. Of these five metals Mo has the largest fission yield for U-fission, although for Pu-fission, Ru and Mo yields are about the same. Through work on fast breeder oxides (U, Pu)O_2 by Davies and Ewart [9], it was soon realised that Mo would not form any oxide in substoichiometric fuel, whereas it could be expected to be completely oxidised in, for example, stoichiometric PuO_2 fuel. In the metallic 'five-metal particles', the concentrations of Mo, Tc, Ru, Rh and Pd were found to vary from particle to particle in the same fuel but — as predicted — the Mo content of the particles was much smaller in PuO_2 than in $PuO_{1.7}$ fuel. Also, a (modified) pattern of MoO_3 was found in X-ray diffraction investigations of microspecimens of irradiated fuel [9].

Since these early studies, the five metal particles have been observed by a variety of methods (optical microscopy, scanning electron microscopy, SEM, and transmission electron microscopy, TEM) in many irradiated fuels as well as in simulated high burnup oxide fuel produced with inactive fission products, the so-called SIMFUEL [10]. Fig. 1 shows typical SEM and TEM pictures of irradiated UO_2 fuels. The SEM image in the upper part of the figure clearly shows five metal particles located within grain boundary fission gas bubbles in the hot central part of the fuel. These precipitates are also found intra-granularly. An example of this is shown in the TEM picture given in the lower part of Fig. 1. The intra-granular particles are usually much smaller than those found at grain boundaries which can reach sizes in excess of 1 μm in fuel that has experienced a power transient during reactor irradiation or which has been annealed in a hot cell following irradiation.

The five metal particles usually exhibit the -Ru (Mo, Tc, Rh, Pd) phase although, less commonly, particles containing two phases have also been observed. The early suggestion that Mo may act as an oxygen buffer was taken up by Johnson and co-workers [11] who proposed Mo/MoO_3 as a (hypothetical) redox couple in (U, Pu)O_2 fuel, assuming that Mo dissolves as Mo^{4+} in the fuel oxide matrix in local equilibrium with Mo in the five metal particles. These authors suggested that electron microprobe analysis (EPMA) determination of the ratio of Mo in solution as an oxide and Mo precipitated as a metal could be used to measure local oxygen potential values. Later work at ITU by Giacchetti and Sari [12], however, indicated a low solubility of Mo in UO_2 (< 250 ppm) and these authors argued that the limited resolution of EPMA would not be able to discriminate submicroscopic precipitates of the type shown in the lower part of Fig. 1 from Mo in solution. These authors also reported that MoO_2 is gaseous at $T \leq 1000°C$ and would be released unless it reacts with, for example, Ba. The most convincing evidence for such a process was recently reported by Tourasse and co-workers [13] in the case of high burnup (U, Pu)O_2 irradiated in the Phenix fast reactor — most to nearly all Mo left the five metal particles at burnups in excess of 7 at.%. This occurred particularly in the hottest parts of the fuel and the released MoO_2 reacted with Cs to form caesium molybdates in the cold part of the fuel. Kleykamp [14] confirmed the low solubility of 'MoO_2' in UO_2 and quoted a value of ≤ 0.006 mol%. The experimental evidence is thus compatible with the following conclusions:

- Mo can act as a buffer for oxygen in stoichiometric oxide fuel, as already explained in Section 1 of this paper (see also refs. [1–3]);
- all Mo is precipitated in five-metal particles in substoichiometric fuel;
- the solubility of Mo in stoichiometric UO_2 is very small.

In contrast, nothing is known about the lattice position of any possible dissolved Mo. The present work aims to fill this gap.

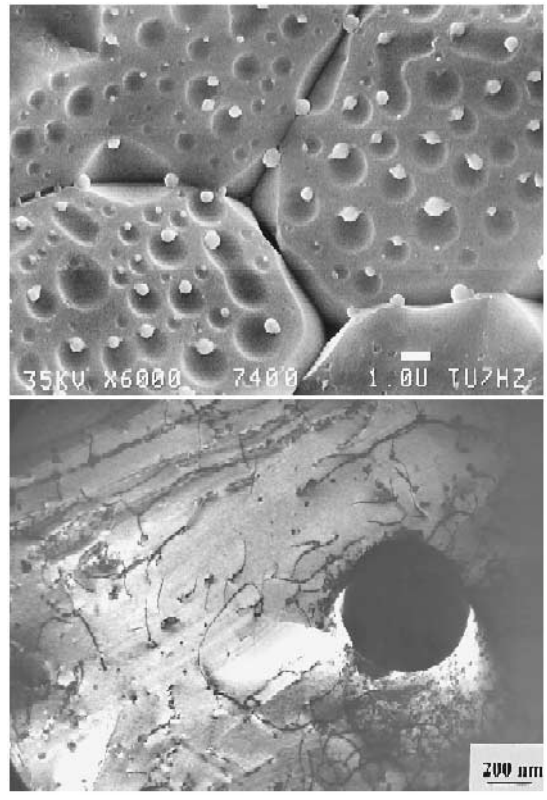

Fig. 1. Electron microscope images of five metal particles in UO_2. The top picture shows an image of a fractured surface revealing grain boundaries with a high density of five metal particles located at bubbles. The lower picture gives a more detailed TEM image of a five metal particle associated with some porosity. Dislocations are punched out to relieve the stress in the lattice around the precipitate.

3. Computational approach

3.1. Methodology

The basic quantities calculated in our computer simulations are the defect formation energies of a number of likely configurations for a single Mo ion in a host UO_2 crystal. The configurations considered are the Mo ion in an interstitial site, in a urania vacancy, in an oxygen vacancy, in a divacancy (a bound oxygen/uranium vacancy pair), in a trivacancy (a bound Schottky trio) and in a tetravacancy (consisting of two oxygen and two uranium vacancies bound together).

The basic defect energies calculated are defined as the difference between the energy of a UO_2 crystal containing one Mo defect or defect complex and the energy of the perfect UO_2 crystal. In the present work only changes in internal energies of defect formation are considered. In general, defect generation may involve several defect species. Indeed, defect equilibria can be modelled by a series of mass action equations which must be solved subject to constraints arising from electroneutrality, impurity concentrations and O/U ratio. The energies of the relevant defect reactions are obtained from the basic defect energies as defined above.

The method used in calculating defect formation energies is well documented and is based on the approach of Mott and Littleton [15,16]. Essentially, interaction energies between ions in the region closest to the defect are summed explicitly. Further away from the defect, the crystal is modelled as a dielectric continuum. This approach has the advantage of reducing summations to a manageable number whilst still allowing the whole crystal to respond to any long range Coulomb interaction due to a charged defect configuration. Atomic interactions are modelled by pair-wise potentials and the ionic model is assumed. Full details of the general approach will be found in Ref. [16] and details of the computer codes used have been reported by Leslie [17]. In the present calculations, the inner, explicitly summed, region contained over 400 ions.

As well as the interactions between pairs of ions, an important feature of the simulations is the modelling of atomic polarisability via the shell model of Dick and Overhauser [18]. In this model, the total charge of the ion is distributed between a core and a massless shell which are harmonically coupled together and the atomic polarisability, α, is given by

$$\alpha = Y^2/k, \tag{1}$$

where Y is the charge on the shell and k is the coupling force constant.

3.2. Interionic potentials and shell model parameters

In addition to the Coulomb interaction between ions, for which formal ion charges are assumed, it is necessary to model the shorter range components of the interaction between two ions arising from Pauli exclusion and van der Waals attraction. A form commonly used to model these latter two components is the Buckingham potential:

$$V = A\exp\left(\frac{-r}{\rho}\right) - \frac{C_6}{r^6}, \tag{2}$$

where r is the distance between the two ions and A, ρ and C_6 are constants to be derived from experiment or by computation. When the shell model is employed, this potential acts between the shells of the ions, thus coupling the polarisability of the ions to the short range interaction.

To describe the interactions between ions in the host UO_2 crystal we employ the potentials of Jackson and co-workers [7]. These are empirically derived potentials which have been used successfully in previous studies of UO_2. For the interactions involving Mo ions, empirical derivation of potentials was not possible. In these cases, van der Waals interactions (incorporated as the C_6 term in the Buckingham potential) were calculated using the formula of Slater and Kirkwood [19] as discussed by Fowler and co-workers [20]. To achieve this, estimates of the ionic polarisabilities were required. Polarisabilities (although unfortunately not in-crystal polarisabilities) have been published for Mo and Mo^{6+} (these where 9 $Å^3$ [21] and 0.26 $Å^3$ [22], respectively). Values for the remaining charge states could not be found in the literature. For the ions Mo^{1+} to Mo^{5+} we thus interpolated between the two known extremes on the basis of the assumption that the polarisabilities scaled with the ionic volume. These estimated polarisabilities were used in deriving both the Mo interaction C_6 values shown in Table 1 and the Mo shell model parameters which are included in Table 2.

In deriving the C_6 parameter, using the approach of Slater and Kirkwood, in addition to the polarisability itself, we require an estimate of the number of electrons significantly contributing to the polarisability. Fowler and co-workers [20] suggest the use of the value derived for the isoelectronic noble gas atom. For Mo^{6+} this would be about 7.3, as derived in Ref. [20] for Kr. For the remaining charge states there is no simple prescription to derive them. We thus fix the electron numbers for all Mo ions at 7. In the Slater and Kirkwood approach however, it is the effect of the polarisability which is most important and the crudity of this estimate for the electron numbers should not have a great effect on the final potentials. We also used this value for the electron number in the shell model, with spring constants being obtained from Eq. (1).

The A and ρ parameters for the various Mo interaction potentials were initially calculated using the electron gas method of Gordon and Kim [23,24]. These potentials formed the basis from which to derive 'empiricised' potentials which are compatible with the empirically derived U^{4+}–O^{2-} potential of Jackson and co-workers [7]. To carry out the empiricisation procedure, the calculated con-

Table 1
Short range potentials used in this study

Interaction	A (eV)	ρ (nm)	C_6 (eV nm^6)	Range (nm)
O^{2-}–O^{2-}	1172.6	0.01363	–	$r < 0.12$
O^{2-}–O^{2-}	–	–	1.34×10^{-4}	$r > 0.26$
U^{4+}–O^{2-}	1518.92	0.038208	6.541×10^{-5}	$r > 0$
U^{3+}–O^{2-}	1142.0	0.04001	5.632×10^{-5}	$r > 0$
U^{5+}–O^{2-}	1612.0	0.03749	4.087×10^{-5}	$r > 0$
U^{6+}–O^{2-}	1839.0	0.03650	3.973×10^{-5}	$r > 0$
Mo–O^{2-}	370.3	0.04417	1.721×10^{-4}	$r > 0$
Mo^{1+}–O^{2-}	345.3	0.04463	6.524×10^{-5}	$r > 0$
Mo^{2+}–O^{2-}	508.3	0.04367	4.308×10^{-5}	$r > 0$
Mo^{3+}–O^{2-}	718.3	0.04102	2.853×10^{-5}	$r > 0$
Mo^{4+}–O^{2-}	914.9	0.03901	1.953×10^{-5}	$r > 0$
Mo^{5+}–O^{2-}	1075.0	0.03764	1.482×10^{-5}	$r > 0$
Mo^{6+}–O^{2-}	1191.0	0.03675	1.013×10^{-5}	$r > 0$
Mo–U^{4+}	4055.0	0.03614	1.2778×10^{-4}	$r > 0$
Mo^{1+}–U^{4+}	3814.0	0.03672	5.176×10^{-5}	$r > 0$
Mo^{2+}–U^{4+}	5324.0	0.03264	3.512×10^{-5}	$r > 0$
Mo^{3+}–U^{4+}	6503.0	0.03038	2.386×10^{-5}	$r > 0$
Mo^{4+}–U^{4+}	7472.0	0.02889	1.668×10^{-5}	$r > 0$
Mo^{5+}–U^{4+}	8366.0	0.02776	1.284×10^{-5}	$r > 0$
Mo^{6+}–U^{4+}	9279.0	0.02682	8.93×10^{-6}	$r > 0$

The Buckingham form $A\exp(-r/\rho)-C_6/r^6$ has been used. For O^{2-}–O^{2-} interactions in the ranges $0.12 < r < 0.21$ nm and $0.21 < r < 0.26$ nm, 5th and 3rd order polynomials, respectively, were used to interpolate between the two ranges quoted in the table. O^{2-}–O^{2-} and U^{4+}–O^{2-} interactions were those derived by Jackson and co-workers [7]. All other interactions were derived during the present study. All short range potentials were cut off for $r > 0.8475$ nm.

tribution from a C_6 term derived from the Slater and Kirkwood formula was subtracted from the U^{4+}–O^{2-} potential of Jackson and co-workers. Then the difference between the electron gas derived potentials for each of the various Mo interactions and a reference electron gas calculated U^{4+}–O^{2-} interaction was obtained. This difference was then used to adjust the modified U^{4+}–O^{2-} potential of Jackson and co-workers, thus giving the final A and ρ parameters for the Mo interactions. This type of approach was originally adopted in the work of Butler and co-workers [25]. The added complexity of deriving C_6 terms separately via the Slater and Kirkwood formula was necessitated by the inability of the electron gas method to model the van der Waals interaction. Interactions for Mo with the charge states 0 through to 6+ were calculated. Also derived using this approach were the interactions involving U^{3+}, U^{5+} and U^{6+}. All of these potentials, which were fitted to the Buckingham form, will be found in Table 1.

Table 2
Shell model parameters used in this study

	Y ($\|e\|$)	k (eV nm^{-2})
O^{2-}	−4.4	29620
U^{4+}	6.54	9424
U^{3+}	6.54	7677
U^{5+}	6.54	11294
U^{6+}	6.54	11680
Mo	7.0	7840
Mo^{1+}	7.0	29400
Mo^{2+}	7.0	49689
Mo^{3+}	7.0	82045
Mo^{4+}	7.0	128289
Mo^{5+}	7.0	176398
Mo^{6+}	7.0	271381

Values for U^{4+} and O^{2-} are those given by Jackson and co-workers [7]. Remaining values are estimates derived in the present study and are based on ionic polarizabilities reported in the literature [21,22].

Table 3
Ionization potentials used in this study

	U (eV)	Mo (eV)
1	–	7.10
2	–	16.15
3	–	27.16
4	31.86	46.40
5	46.57	61.25
6	61.70	68.00

Sources are Refs. [21,29].

The ionisation potentials used in the model when accounting for charge transfer effects have been taken from the literature and are tabulated in Table 3.

3.3. Analysis of results

There are three parameters of principal importance employed in analysing the results from our simulations: fission product concentration, fuel stoichiometry (O/U ratio) and temperature. As noted earlier the energy terms calculated in our simulations are internal energy changes and these do not include any temperature dependence except that they are based on potentials for the UO_2 lattice designed to give a good value for the lattice parameter over a broad range of temperatures (see Ref. [7]). It should be noted however, that in the mass action approach adopted in analysing our results, some temperature dependence is introduced through the configurational entropy terms. Both the temperature variation of defect energies, as well as the change in vibrational entropy of the lattice brought about by the creation of a defect, can in principle be calculated but we have not attempted this in the present work. In view of this we do not explicitly investigate the effect of temperature variation on Mo behaviour although there are undoubtedly some interesting temperature dependency effects to be found for some of the fission products. In these calculations we thus fix the temperature used in solving the mass action equations at a value of relevance to much of the experimental literature and investigate changes in

Mo behaviour brought about by variations in O/U ratio and Mo concentration alone.

The mass action approach adopted in the present work is essentially the same as that outlined by Lidiard [26], which involves minimising the chemical potentials of all the defect configurations under consideration in this paper, subject to the system constraints (electroneutrality, Mo concentration and O/U ratio).

4. Results

The basic defect energies calculated are reported in Table 4. For the calculations concerning Mo^{3+} in a trivacancy site and Mo^{1+} in an oxygen vacancy, convergence difficulties were initially experienced but these were removed if the calculations were repeated with rigid ion representation of the relevant Mo species (the shell model still being employed for the host lattice ions). By calculating and comparing defect energies of several Mo defects with and without shells on the Mo, it was confirmed that the act of removing the shell from the Mo ions would have only a small effect on calculated defect energies (probably of the order of a few tenths of an eV for the problem configurations) and thus removing the Mo shells in the two problem cases should have little influence on the final results. Difficulties also occurred in eight other calculations for which convergence could not be obtained. Subsequent analysis, however, showed that the Mo charge states involved in these configurations will not be present in significant concentrations.

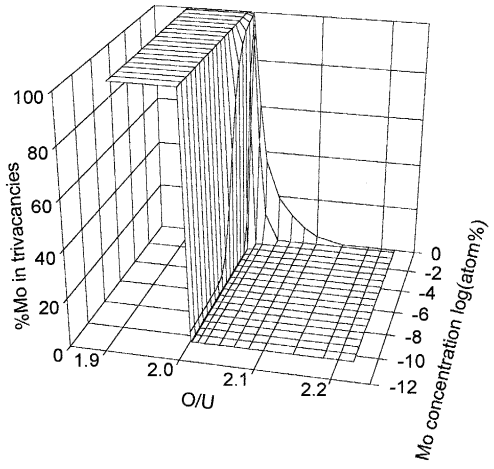

Fig. 2. The percentage of single Mo atoms occupying trivacancy sites as a function of O/U ratio and Mo concentration. Only neutral Mo atoms are calculated to be present in trivacancies.

Table 4
Calculated defect formation energies for Mo in UO_2

Defect	Energy (eV)	Defect	Energy (eV)
O^{2-} interstitial	−12.26	trivacancy	110.47
V_O	17.08	tetravacancy	187.69
V_U	80.22	U^{3+} at V_U	35.25
Divacancy	94.87	U^{5+} at V_U	−46.04
		U^{6+} at V_U	−105.23
Mo^0 at V_U	82.66	Mo^0 at divacancy	97.01
Mo^{1+} at V_U	74.80	Mo^{1+} at divacancy	89.82
Mo^{2+} at V_U	58.49	Mo^{2+} at divacancy	74.31
Mo^{3+} at V_U	31.51	Mo^{3+} at divacancy	47.89
Mo^{4+} at V_U	−6.75	Mo^{4+} at divacancy	9.46
Mo^{5+} at V_U	−57.98	Mo^{5+} at divacancy	–
Mo^{6+} at V_U	−122.69	Mo^{6+} at divacancy	–
Mo^0 at V_O	26.61	Mo^0 at trivacancy	112.14
Mo^{1+} at V_O	24.90	Mo^{1+} at trivancancy	105.74
Mo^{2+} at V_O	11.85	Mo^{2+} at trivancancy	91.29
Mo^{3+} at V_O	–	Mo^{3+} at trivancancy	65.53
Mo^{4+} at V_O	–	Mo^{4+} at trivancancy	27.23
Mo^{5+} at V_O	–	Mo^{5+} at trivancancy	−26.64
Mo^{6+} at V_O	–	Mo^{6+} at trivancancy	−98.88
Mo^0 interstitial	11.76	Mo^0 at tetravacancy	188.71
Mo^{1+} interstitial	8.81	Mo^{1+} at tetravacancy	183.06
Mo^{2+} interstitial	−5.70	Mo^{2+} at tetravacancy	169.53
Mo^{3+} interstitial	−31.78	Mo^{3+} at tetravacancy	146.60
Mo^{4+} interstitial	−70.55	Mo^{4+} at tetravacancy	111.47
Mo^{5+} interstitial	−122.66	Mo^{5+} at tetravacancy	–
Mo^{6+} interstitial	−188.52	Mo^{6+} at tetravacancye	–

Quoted energies are with respect to the relevant ions at infinity. Also included in the table are the energies of formation of some other important intrinsic defects. The calculated lattice energy for UO_2, which is also required in the analysis of the results, was 103.14 eV. V_U and V_O denote the uranium and oxygen vacancies, respectively, and Mo^0 at V_U denotes a neutral Mo atom substitutional at a uranium site.

By fixing the system temperature at 1673 K and using the results of Table 4, it was possible to determine the defect equilibrium under variations in O/U ratio and concentration of single atoms of Mo. Results are summarised in Figs. 2–7. As metallic and oxide Mo precipitates are not included when solving the mass action equations, this procedure corresponds to investigating the nature of the Mo dispersed throughout the UO_2 lattice as isolated single atoms. The matter of Mo precipitation will, however, be discussed towards the end of this paper.

We plot in Fig. 2 the calculated variation in the proportion of Mo located as neutral atoms in trivacancies, over the whole range in stoichiometry and concentration being considered. In sub-stoichiometric UO_{2-x} it is clear that trivacancies are the dominant site for single Mo atoms at all degrees of sub-stoichiometry and Mo concentrations and that, consistent with experimental studies (see Section 2), no oxidation of Mo occurs. Fig. 2 also shows that, in addition to its dominance as a Mo site in UO_{2-x} (where it accommodates almost 100% of the Mo), the trivacancy would also appear to play a role in UO_{2+x} when the Mo

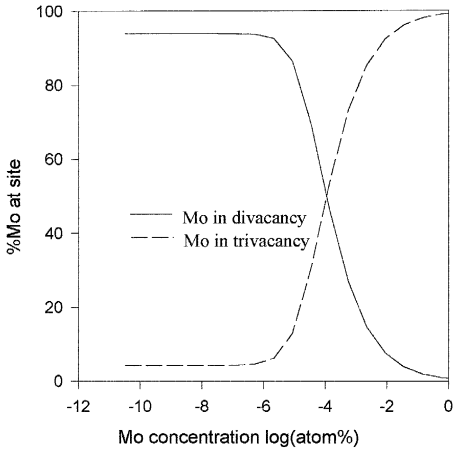

Fig. 3. The percentage of single Mo atoms in di- and trivacancy sites as a function of Mo concentration in UO_2 of stoichiometric composition. Only neutral Mo atoms are calculated to be present in these sites.

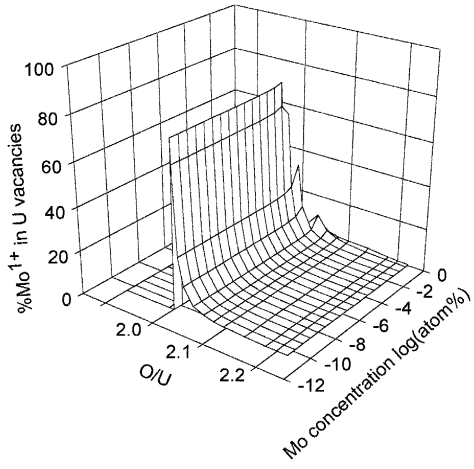

Fig. 5. The percentage of single Mo atoms present as Mo^{1+} in isolated uranium vacancies as a function of O/U ratio and Mo concentration.

concentration is particularly high. We shall return to a discussion of this point later.

In Fig. 3 it is shown that in stoichiometric UO_2 the importance of the trivacancy is strongly dependent upon the Mo concentration. This finding may be compared to the results of calculations on Xe in UO_2 where a similar behaviour was found [27]. At low concentrations ($\leq 10^{-6}$ at.%), relatively little Mo should be found in trivacancies (of the order of 5% of the total Mo concentration). At high concentrations, however, the proportion of Mo in trivacancies should approach that calculated for the case of UO_{2-x}. Whenever Mo is present in a trivacancy site it is calculated to be in the neutral charge state.

In plotting Fig. 3, we have used the definition of stoichiometric composition as an O/U ratio equal to 2 *exactly*. In practical applications the stoichiometry will only be determinable to within certain bounds and it is important to remember that it may be most appropriate to compare experimental data referring to nominally stoichiometric urania with calculations on a system with an O/U ratio only approximately equal to 2. We shall find that at low Mo concentrations this distinction is significant.

Also shown in Fig. 3 is the proportion of Mo present as neutral atoms in stoichiometric UO_2 in divacancy sites. The trivacancy and divacancy sites are calculated to account for almost all the single Mo atoms at exactly stoichiometric composition. It will be seen that for concentrations less than about 10^{-6} at.% over 90% of the Mo is located at divacancy sites. Above this concentration, the

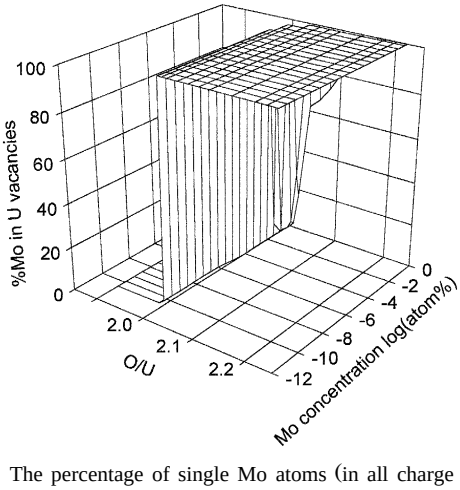

Fig. 4. The percentage of single Mo atoms (in all charge states) present in isolated uranium vacancies as a function of O/U ratio and Mo concentration.

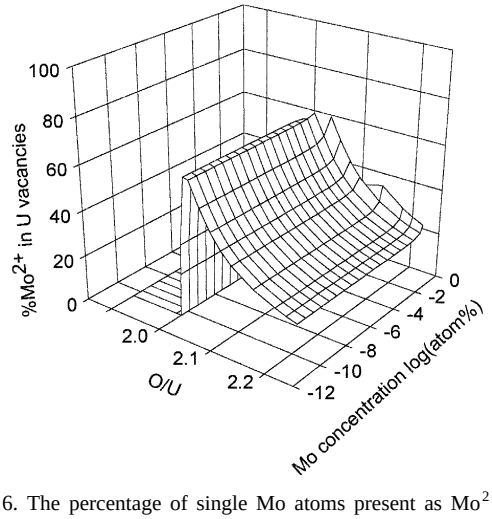

Fig. 6. The percentage of single Mo atoms present as Mo^{2+} in isolated uranium vacancies as a function of O/U ratio and Mo concentration.

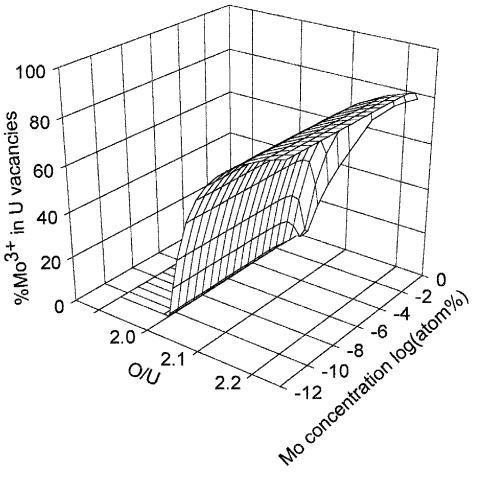

Fig. 7. The percentage of single Mo atoms present as Mo^{3+} in isolated uranium vacancies as a function of O/U ratio and Mo concentration.

trivacancy site gradually regains its importance as the Mo concentration increases up to and into the region where the model of isolated, non-interacting defects, assumed in the mass action approach, becomes less accurate.

For hyperstoichiometric compositions it is found that ionisation of Mo becomes an important process. The location of the Mo also undergoes a radical change in that the single uranium vacancy becomes the dominant site. We show this in Fig. 4 where we have plotted the proportion of Mo in uranium vacancies (all charge states) as a function of the O/U ratio and Mo concentration.

From Fig. 4 we can see why it is important to distinguish the idealised exact stoichiometric composition O/U $= 2$ discussed above, from the nominal stoichiometric composition of experimental work. Although at high Mo concentrations a gradual change in the behaviour of Mo is calculated, at low concentrations the change in behaviour on passing from UO_{2-x} through UO_2 to UO_{2+x} is abrupt. We can illustrate this by considering the behaviour of Mo in $UO_{2.001}$, slightly hyperstoichiometric urania. In this case we find that at low concentrations all the Mo is located in single uranium vacancies. Not until the concentration exceeds 10^{-3} at.% does the behaviour begin to resemble that of exactly stoichiometric UO_2 (that is, the region where neutral Mo at di- and trivacancies is prevalent). As already mentioned, our models based on isolated defects become, in any case, less accurate at such high concentrations. Clearly then, it will be difficult to be sure which of our regions of composition it would be appropriate to compare with the experimental data on nominally stoichiometric urania. Small differences in composition (that is O/U ratio) are seen to lead to quite different predictions for Mo behaviour.

One interesting and perhaps surprising result from our calculations concerns the possible charge states of Mo in urania. In Figs. 5–7 we decompose Fig. 4 into the proportions of Mo present in uranium vacancies in the charge states $1+$, $2+$ and $3+$ — the three charge states which prevail in UO_{2+x}. As a general rule, increases in hyperstoichiometry lead to increased Mo ionisation, which, however, does not extend beyond Mo^{3+}. In $UO_{2.001}$ for low Mo concentrations, Mo^{1+} is a dominant state. As the degree of hyperstoichiometry is increased it is Mo^{2+} and finally Mo^{3+} which dominates. Up to quite high Mo concentrations in $UO_{2.2}$ for example, over 80% of the isolated Mo is calculated to be present as Mo^{3+} in uranium vacancies. Importantly, however, our calculations do not suggest further ionisation to Mo^{4+} or higher charge states — a surprising result as it is often assumed that isolated Mo may be present as Mo^{4+} substituting at uranium vacancies (see for example [28]). We return later to a discussion of the reasons behind this result.

5. Defect reactions and mechanisms

Having analysed results of our calculations on the behaviour of single atoms of Mo in urania, we now consider in detail some of their mechanistic implications. In UO_{2-x} neither the oxygen vacancy nor the interstitial site are calculated to be favourable locations for Mo. Although both sites are readily available, the calculated defect energies do not favour these sites in preference to the neutral trivacancy. In particular, we can calculate the energies of the reactions

$$Mo_{trivacancy} + U_U + 2O_O \rightarrow Mo_i \quad \Delta U \simeq 2.7 \text{ eV} \tag{3}$$

$$Mo_{trivacancy} + V_O^{\cdot\cdot} + U_U + 2O_O \rightarrow Mo_O^{\cdot\cdot} \quad \Delta U \simeq 0.5 \text{ eV}, \tag{4}$$

where we have employed Kröger–Vink notation in which Mo_i and $Mo_O^{\cdot\cdot}$ are neutral Mo atoms at interstitial and oxygen vacancy sites respectively, and $V_O^{\cdot\cdot}$ is a vacant oxygen site. In these and subsequent defect reaction equations, ΔU is the internal energy change associated with the reaction. The last of the two processes shown above, where the accommodation of Mo at pre-existing oxygen vacancies competes with accommodation at trivacancy sites, is almost viable and, within the bounds of the approximations used in the calculations, it cannot be ruled out that the oxygen vacancy has some role to play as a site for Mo in UO_{2-x}.

In exactly stoichiometric UO_2, the divacancy is the dominant site for Mo:

$$Mo_{trivacancy} + O_i \rightarrow Mo_{divacancy} \quad \Delta U \simeq -2.5 \text{ eV}. \tag{5}$$

The process shown in Eq. (5) is however limited through the Frenkel equilibrium reaction; there is not an infinite supply of oxygen interstitials. In particular, if the concentration of Mo becomes large, the process described by Eq.

(5) will no longer be able to play its full role and it may be expected that an increasingly larger fraction of the Mo will remain in trivacancies; the behaviour is shown in Fig. 3.

An important point to bear in mind when considering the significance that di- and trivacancy sites have for Mo location is that, at all values of O/U ratio, the concentration of empty di- and trivacancy sites in urania is extremely small. When such sites are calculated to be important locations for Mo, it is therefore best to consider the Mo ion as causing the creation of the relevant site around itself, rather than simply locating itself at a pre-existing trap site — a process which is unlikely to occur.

As we increase the degree of hyperstoichiometry, we introduce excess extrinsic oxygen into the lattice. The evidence, from both experiment and computation, that this oxygen is accommodated as oxygen interstitials is overwhelming. With the availability of an extrinsic supply of oxygen interstitials in UO_{2+x}, a second reaction path becomes readily available, allowing single uranium vacancies to form the majority sites for the Mo:

$$Mo_{\text{divacancy}} + O_i \rightarrow Mo_U \quad \Delta U \simeq -2.4 \text{ eV}. \tag{6}$$

However, as the concentration of Mo increases the oxygen interstitial supply will become unable to sustain this process and at high concentrations divacancies and trivacancies again dominate.

In practice, the calculations show that a neutral Mo atom at a uranium vacancy is not a particularly populous defect at any O/U ratio. To understand why, we need to consider the effect of O/U ratio on charge transfer reactions.

In our model we employ an atomistic picture of localised charge carriers. Thus, if we consider the transfer of an electron from a neutral Mo atom to the UO_2 lattice we may write an equation such as

$$Mo + U^{4+} \rightarrow Mo^{1+} + U^{3+}, \tag{7}$$

where the charge on a lattice uranium is reduced from the formal charge of $4+$. Had there been a population of U^{5+} ions we could have written

$$Mo + U^{5+} \rightarrow Mo^{1+} + U^{4+}. \tag{8}$$

Using our calculated defect energies for U^{3+} and U^{5+} at normal lattice sites and tabulated ionisation potentials for the free ions (these data will be found in Tables 4 and 3) we find that of the two processes, the second is more favourable by about 3.9 eV. This is important, for if we consider the ionisation of Mo located in a uranium vacancy for example, we find that the first of these two processes is not viable but the second is.

As the degree of hyperstoichiometry is increased the lattice needs not only to accommodate the excess oxygen (as O^{2-} interstitials), it must also retain electroneutrality. The model we use for this, is the process

$$O_2 \overset{UO_2}{\rightarrow} 2O_i'' + 4h^{\cdot}. \tag{9}$$

The symbol $h^{\cdot}$ denotes a hole which, in our model of localised charges, must be located on a localised species in the system. In pure urania (no fission products) one possibility is the creation of U^{5+} ions. Another is the creation of U^{6+} ions. Using our calculated defect energies and the tabulated ionisation energies we find that, in agreement with the previous work of Catlow [4], U^{5+} ions are the most likely means of retaining electroneutrality. It should be remembered that the errors in the data are significant and U^{6+} may still be an important charge state in urania. What is important here, however, is the point that increasing oxygen excess leads to an increased hole concentration and the release of more favourable paths for the ionisation of Mo. We thus find, for example, that in $UO_{2.001}$ most of the isolated Mo is present as Mo^{1+} whereas in $UO_{2.2}$ Mo^{3+} is the most populous state. The location of Mo at U vacancies in UO_{2+x} is thus associated with ionisation of the Mo.

As it is such an important point, we should look in detail at the process of ionisation of Mo at the uranium vacancy site:

$$Mo_U^{(n-1)} + + U_U^{5+} \rightarrow Mo_U^{n+} + U_U^{4+}. \tag{10}$$

When calculating the change in internal energy ΔU of this process, it is useful to divide this energy change into two components; the change in energy due to a change in defect types ΔD and the change due to charge transfer from $Mo^{(n-1)+}$ to U^{5+}, ΔIP. This last component is estimated as the 5th ionisation potential of uranium subtracted from the nth ionisation potential of Mo. These two components together with the total energy change are plotted in Fig. 8 for values of n from 1 to 6. We see a steady decrease in ΔD with increasing n due to the higher

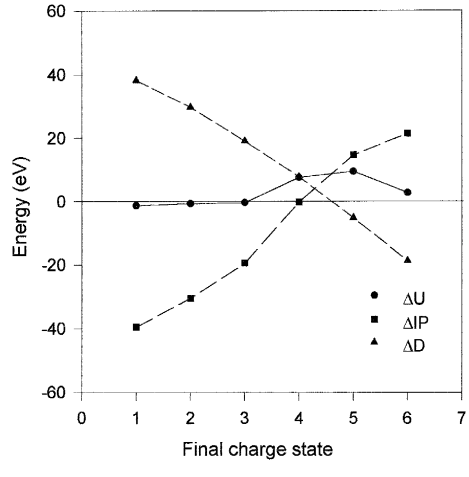

Fig. 8. A breakdown of the energy contributions to Mo charge transfer reactions of the form shown in Eq. (10). Where the final charge on the Mo ion is less than $4+$ the total internal energy changes for these reactions are negative. ΔU is the total internal energy change, ΔD and ΔIP are defined in the text.

charge and smaller ionic radius of Mo. The increase in ΔIP is, however, well known to be non-linear and the jump in ΔIP at $n = 4$ pushes ΔU well into the positive range when attempting to form Mo^{4+} (and indeed Mo^{5+} and Mo^{6+}). This is the reason why, within the approximations inherent in our model, Mo^{4+} ions at uranium vacancies do not form.

The approach used above, of adopting a model of localised charge carriers, was followed in order to produce a scheme in which all ions are dealt with in a consistent manner. Such an approach, however, is not without its problems. For example, it is unreasonable to expect that the ionisation potentials for free ions will provide an accurate measure of the energy of ionisation for ions within a solid. In particular, the calculated formation energies of the U^{3+} and U^{5+} ions may not be fully consistent with the electronic structure of UO_2 and the predicted thermal band gap of 3.9 eV is significantly larger than that estimated from experimental work. As an alternative approach to that adopted in the present work, in their study of a variety of fission products in UO_2, Grimes and Catlow [6] used the model of localised charge carriers for the fission products but avoided the approach when dealing with uranium ions. They assumed that the conduction band in UO_{2-x} was close to the vacuum level and that the electron affinity of the lattice (with electrons being added to the conduction band) could be taken as zero. In UO_{2+x} (with hole states present in the valence band) they assumed electrons would be added to the valence band and that the appropriate electron affinity of the lattice would be higher than was the case for UO_{2-x} by the value of the thermal band gap of UO_2. The appropriate value for the electron affinity of stoichiometric UO_2 was taken to be intermediate between the values used for UO_{2-x} and UO_{2+x}. Although such an approach has not been adopted in the present work, it is worth noting that the qualitative results reported here for the location of Mo in UO_{2-x} and UO_{2+x} would have remained unchanged had the method of Grimes and Catlow been employed. Additionally, although Mo would be more readily oxidised in UO_{2+x}, Mo^{4+} would still not be predicted to occur.

Returning to the present study, a parameter that is also of interest is the free energy change that occurs when Mo is added to a crystal of previously pure urania. It has been shown above that the location of Mo in the lattice (assuming that precipitation does not occur) is dependent on both the composition of the urania (O/U ratio) and the amount of Mo present. There is therefore a distribution of Mo in various states where the population of each state depends upon these two parameters. Once Mo has been added, an approximation to the difference in the (Helmholtz) free energy of the crystal with and without Mo is given by a weighted sum of the energies and configurational entropies of these states together with any contributions arising from a change in the intrinsic defect populations (for example a change in the number of oxygen interstitials). It should be emphasised that in our estimate of the defect entropy only configurational terms have been included; vibrational entropy terms have been neglected. The free energy change, ΔA, calculated is equivalent to that associated with the reaction

$$\mathrm{cMo}(\ ) + \mathrm{UO}_{2+y}(\mathrm{s}) \rightarrow (\mathrm{U}, \mathrm{Mo}_{\mathrm{c}})\mathrm{O}_{2+y}(\mathrm{s}), \qquad (11)$$

where Mo( ) signifies an Mo atom at infinity. It should be noted that Eq. (11) refers to a closed system and that this is an additional source of error when our calculated ΔA is compared to results relating to an open system of experimental work where the oxygen potential is a main controlling parameter.

In Fig. 9 we have plotted ΔA per Mo atom as a function of the O/U ratio and Mo concentration. For convenience ΔA has been plotted only for the region $\Delta A \geq 0$. When $\Delta A > 0$ the reverse of Eq. (11) will be spontaneous and Mo in the gas phase will be favoured above Mo in solution in UO_{2+y} (where y takes positive and negative values). When $\Delta A < 0$ the forward direction of Eq. (11) is preferred and solution of Mo in UO_{2+y} is favoured above the gaseous state.

The value of ΔA is easily related to the Mo behaviour already discussed and shown principally in Figs. 2 and 4. In UO_{2-x}, where Mo is located exclusively in trivacancies, the energy change is large and positive, indicative of an insoluble nature for Mo. In UO_{2+x} however, we find that the location of Mo in uranium vacancies may (dependent upon Mo concentration) result in Mo in solution being favoured above Mo in the gaseous state. Fig. 9 indicates, however, that even at O/U ratios most favourable to Mo solubility, less than 10^{-4} at.% Mo will

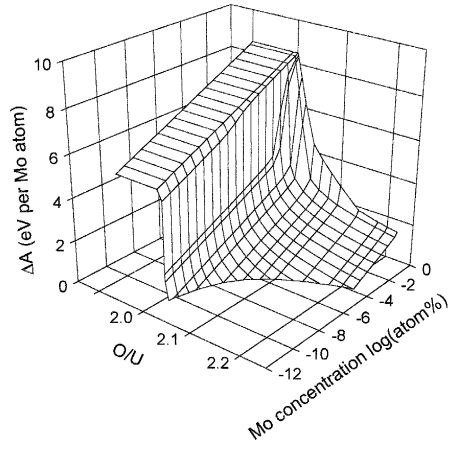

Fig. 9. Plot of the approximate free energy change ΔA occurring when single Mo atoms in the gas phase are added to pure urania at a fixed O/U ratio. Only the region $\Delta A > 0$ is shown. In this region precipitation or high release of Mo is favoured. When the plot cuts the $\Delta A = 0$ plane and becomes negative, solution of Mo in urania is preferred over Mo in the gas phase. However, Mo precipitation is still possible.

be soluble in urania. This figure for the maximum solubility is likely to be strongly influenced by the exact nature of the particular closed system under examination.

We can further consider the reaction

$$(\mathrm{U, Mo_c})\mathrm{O}_{2+y}(\mathrm{s}) \rightarrow \mathrm{UO}_{2+y}(\mathrm{s}) + \mathrm{cMo(s)}, \qquad (12)$$

where the metal phase of Mo is produced. This process can be used as an approximation for the precipitation of Mo into the five-metal particles. The energy change associated with this reaction may be approximately written as $-(\Delta A + \Delta A_{\mathrm{sub}})$ where ΔA is the free energy change of Eq. (11) and ΔA_{sub} is the free energy change upon sublimation of metallic Mo. The enthalpy of sublimation of Mo over a wide temperature range is about 6.5 to 6.8 eV per atom [21] and the free energy change associated with sublimation, though less than this, is probably still quite substantial (and positive). Hence, precipitation will be favoured for those regions of the ΔA plot in Fig. 9 with values $(\Delta A + \Delta A_{\mathrm{sub}}) > 0$.

At large degrees of hyperstoichiometry and small Mo concentrations (the most favourable solubility conditions calculated for single Mo atoms) the calculated free energy change on adding Mo is never much less than -1 to -2 eV. Hence even in the regions of concentration and O/U ratio most favourable to solution of Mo in urania, precipitation is likely to be preferred. This precipitation may be into a metallic form as discussed here. However, it is also in the high hyperstoichiometry region that the oxygen potential favours the formation of various oxide precipitates and the formation of these phases has not been considered in this paper. Precipitates would thus be likely to form over the whole stoichiometry range, providing the kinetics of this does not provide a barrier.

6. Summary

The calculations presented in this paper have concentrated on the location and charge state of *those Mo atoms dispersed throughout the urania lattice*, for which we can conclude

- In UO_{2-x}, Mo will be present as neutral atoms in trivacancy sites.
- In UO_2, Mo will be present as neutral atoms in di- and trivacancy sites with perhaps a minor amount located in single uranium vacancies.
- In UO_{2+x}, Mo will be found principally in single uranium vacancies with charge states from 0 to $3+$. Increased ionisation of Mo is related to increases in O/U ratio.

A plot of the approximate free energy change associated with adding Mo atoms in the gaseous state to urania suggests that this process is only favourable at low Mo concentrations in UO_{2+x}. A similar process where the Mo begins in the metallic state is probably not favoured at any stoichiometry and hence precipitation of Mo in urania is likely, as is experimentally observed. The oxygen potential buffering effect of Mo in urania, in part at least, originates from the oxidation of that dispersed population of Mo focused upon in this paper. Further buffering has been recently shown to occur by oxidation of Mo in the metal precipitates [30]. On the basis of the results given here and further work, it should be possible to calculate the amount and average charge state of Mo in the lattice as a function of burnup and hence test whether the present results are in agreement with the recent experimental measurements of one of the authors [3].

Acknowledgements

The authors thank A.H. Harker and Harwell Laboratory for permission to use several of the computer codes employed in this work. S.N. acknowledges the grant of a PhD fellowship within the Human Capital and Mobility Programme of the European Commission. I.L.F. Ray and H. Thiele are thanked for the SEM and TEM images in Fig. 1.

References

[1] H. Kleykamp, J. Nucl. Mater. 131 (1985) 221.
[2] H. Kleykamp, J.O. Paschoal, R. Pejsa and F. Thümmler, J. Nucl. Mater. 130 (1985) 426.
[3] Hj. Matzke, J. Nucl. Mater. 223 (1995) 1.
[4] C.R.A. Catlow, Proc. R. Soc. London A353 (1977) 533.
[5] C.R.A. Catlow, Proc. R. Soc. London A364 (1978) 473.
[6] R.W. Grimes and C.R.A. Catlow, Philos. Trans. R. Soc. London A335 (1991) 609.
[7] R.A. Jackson, A.D. Murray, J.H. Harding and C.R.A. Catlow, Philos. Mag. A53 (1986) 27.
[8] B.T. Bradbury, J.T. Demant and P.M. Martin, UKAEA report AERE-R 5149 (1966).
[9] J.H. Davies and F.T. Ewart, J. Nucl. Mater. 41 (1971) 143.
[10] P.G. Lucuta, R.A. Verrall, Hj. Matzke and B.J. Palmer, J. Nucl. Mater. 178 (1991) 48.
[11] I. Johnson, C.E. Johnson, C.E. Crouthamel and C.A. Seils, J. Nucl. Mater. 48 (1973) 21.
[12] G. Giacchetti and C. Sari, Nucl. Technol. 31 (1976) 62.
[13] M. Tourasse, M. Boidron and B. Pasquet, J. Nucl. Mater. 188 (1992) 49.
[14] H. Kleykamp, J. Nucl. Mater. 206 (1993) 82.
[15] N.F. Mott and M.J. Littleton, Trans. Faraday Soc. 34 (1938) 485.
[16] C.R.A. Catlow and W.C. Mackrodt, in: Computer Simulation of Solids, eds. C.R.A. Catlow and W.C. Mackrodt (Springer, Berlin, 1982).
[17] M. Leslie, S.E.R.C. Daresbury Laboratory report, DL/SCI/TM31T (1982).
[18] B.G. Dick Jr. and A.W. Overhauser, Phys. Rev. 112 (1958) 90.
[19] J.C. Slater and J.G. Kirkwood, Phys. Rev. 37 (1931) 682.
[20] P.W. Fowler, P.J. Knowles and N.C. Pyper, Molec. Phys. 56 (1985) 83.
[21] Gmelin Handbook of Inorganic Chemistry, 8th Ed. (Springer, 1983, 1985).

[22] W.R. Johnson, D. Kolb and K.N. Huang, At. Nucl. Data Tables 28 (1983).
[23] R.G. Gordon and Y.S. Kim, J. Chem. Phys. 56 (1972) 3122.
[24] J.H. Harding and A.H. Harker, UKAEA report AERE-R-10425 (1982).
[25] V. Butler, C.R.A. Catlow and B.E.F. Fender, Radiat. Eff. 73 (1983) 273.
[26] A.B. Lidiard, in: Crystals with the fluorite structure, ed. W. Hayes (Clarendon, Oxford, 1974).
[27] S. Nicoll, Hj. Matzke and C.R.A. Catlow, J. Nucl. Mater. 226 (1995) 51.
[28] D.R. Olander, Fundamental Aspects of Nuclear Reactor Fuel Elements (Energy Research and Development Administration, 1976).
[29] CRC Handbook of Chemistry and Physics, 65th Ed. (CRC, Boca Raton, FL, 1984).
[30] P.C. Lucuta, Hj. Matzke and D.S. Cox, to be published in J. Nucl. Mater.